

On the Initial Imperfections and Their Relations to the Strength of Webplates of Actual Steel Bridges

By

Yoshiji NIWA*, Eiichi WATANABE**, and Yoshitaka IWASHIMIZU***

(Received December 27, 1980)

Abstract

This study is mainly concerned with statistical investigations on the actual initial imperfections and their relations to the load carrying capacities of the webplates of steel bridges.

The basic data to be used throughout the study have been collected by the Initial Deflection Measurement Committee, IDMC, of the Society of Steel Construction of Japan, abbreviated as JSSC.

In order to show what types of webplate systems are covered throughout the study, various statistical information on the mechanical and geometric parameters is firstly presented, and then, various kinds of the initial imperfections existing in the actual steel bridges are subjected to statistical considerations.

Through the statistical analyses, the probabilities of exceedance of various imperfections are evaluated. From these fractile values, some comments on the regulations of the initial imperfections by the current design codes are drawn.

1. Introduction

In this country, the specifications on the design and fabrication of steel bridges have been mostly based on the linear structural analysis and the conventional design method termed as "allowable stress design". Through remarkable advancements and innovations in nonlinear structural analysis and practical engineering, steel bridges seem to have been designed and fabricated with significantly improved precision and certainty. Without doubt, the fact that the new concept, termed as the "ultimate strength design" method is steadily replacing the conventional design method, can be thought of as reflecting these advancements.

The ultimate strength of steel bridges is generally considered to be significantly affected by inevitable yet uncertain factors including the geometric initial imper-

* Dr. Eng., Professor of Civil Engineering,

** Ph. D., Associate Professor of Civil Engineering,

*** Graduate Student of Civil Engineering, Kyoto University.

fections, eccentricities, and the residual stresses.

In order for the ultimate strength design to be adopted for design practice, it is necessary to provide sufficient information about these rather random factors. In this view point, IDMC set forth a new program of investigations on the actual distributions of the geometric imperfections of steel bridges under construction a few years ago. This program of study involved many organizations such as universities, official authorities, steel makers, and fabricators of steel bridges.¹⁾

The analyses of the measured data were undertaken by Kyoto University, Osaka University, and Osaka City University. Kyoto University was particularly responsible for the data pertaining to the webplates of the steel bridges.

The webplates considered herein consist of web panels, horizontal stiffeners, vertical stiffeners, and flanges, as shown in Fig. 1. The types of the steel bridges under consideration were limited to the composite I-girders, composite box-girders, I-girders with orthotropic slabs, and box-girders with orthotropic slabs.

The measurements were performed at the center of the span, and at the quarter points in the case of simply supported bridges; while they were performed at the central points of the subspans and on the intermediate supports in the case of continuously supported bridges.

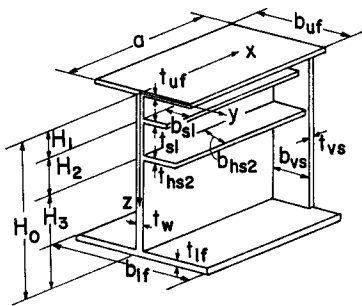


Fig. 1. The webplate system.

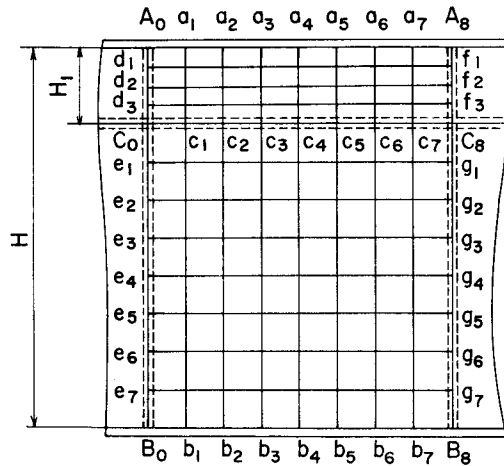


Fig. 2. The sets of measured points.

The measurement can be explained by Fig. 2. It consists of the following sets of measured points:

- (1) Intersections of the vertical stiffeners with the horizontal stiffeners and the flanges (Points $A_0, A_8, B_0, B_8, C_0,$ and C_8),

- (2) Intersections of the webplate with the flanges and stiffeners (Points $A_0, a_1, \dots, a_7, A_8; B_0, b_1, \dots, b_7, B_8; C_0, c_1, \dots, c_7, C_8$),
- (3) Intersections of the webplate with the vertical stiffeners (Points $A_0, d_1, \dots, d_3, C_0, e_1, \dots, e_7, B_0; A_8, f_1, \dots, f_3, C_8; g_1, \dots, g_7, B_8$),
- (4) Grid points of web panels (mesh points 4×8 for $H_1 < 40$ cm; 8×8 for $H_1 \geq 40$ cm, and for $H - H_1$),
- (5) Grid points on the horizontal stiffener (Points $C_0, c_1, \dots, c_7, C_8$).

The measurements corresponding to items (1)~(4) are concerned with the initial displacements in the y-direction, and that corresponding to item (5) is concerned with the initial displacements in the z-direction, respectively referring to Fig. 1.

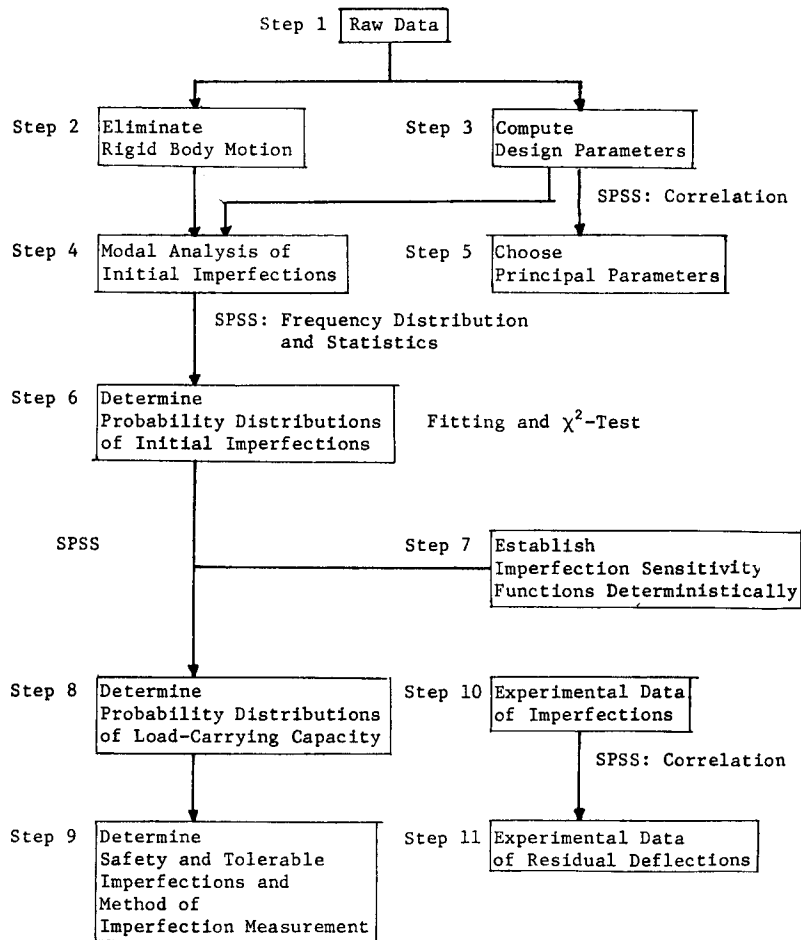


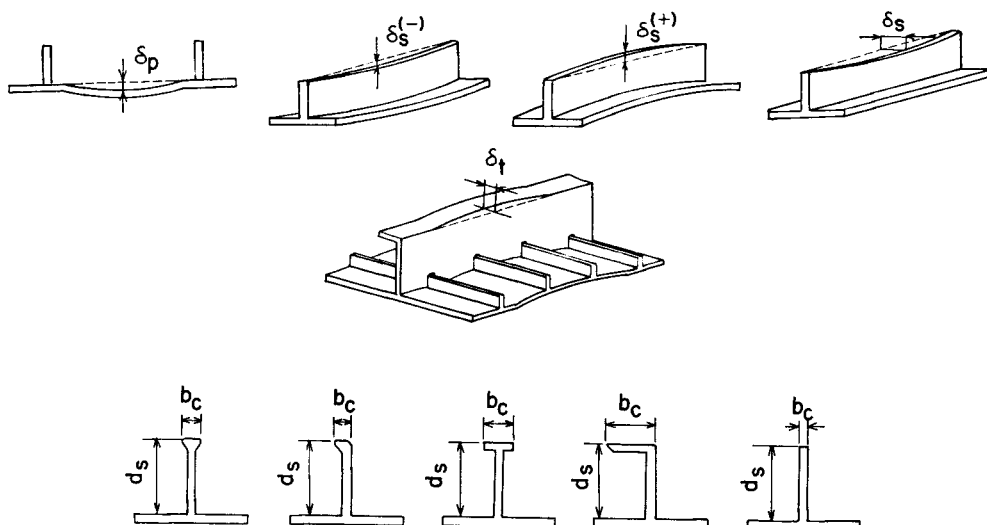
Fig. 3. The general flow chart of the proposed study.

Table 1. The limitation of the imperfections by the design specifications.

| | | IDWR ³⁾ (1973) | AASHTO ⁴⁾ (1977) | ÖNORM* (1975) | DAST-Rit 012 ⁵⁾ (1978) | JSHB (1973) ²⁾ |
|------------------------|------------------|---|---|--|---|--|
| WEB PANEL | δ_p | $\frac{G}{30t} \left(1 + \frac{b}{5000}\right)$ mm for $t < 25$ mm $\frac{G}{750} \left(1 + \frac{b}{5000}\right)$ mm for $t \geq 25$ mm but no less than 1 mm in flange and diaphragm panels and in unrestrained web panels in compression 3 mm in other web panels [G: the gauge length] longitudinal direction- $G=2b$ where $a > 3b$ $G=a$ where $a < 3b$ transverse direction- G =the greatest length practicable within stiffeners spacing b | 4.8 mm or $\frac{0.159D}{144\sqrt{T}}$ m, whichever is the greater D: the least dimension in (m) along the boundary of the panel T: the minimum thickness in (m) of the plate comprising the panel | $\frac{b}{250}$ or 4 mm, whichever is the lesser | $\frac{a}{250}$ or $\frac{b}{250}$, whichever is the lesser | for flanges, box-girders, and steel deck plates $\frac{b}{150}$ for beam panels $\frac{b}{250}$ |
| LONGITUDINAL STIFFENER | $\delta_s^{(-)}$ | $\frac{l_s}{1200}$ or 2 mm whichever is the greater $G=l_s$: the length of the stiffener or rib between cross members, webs, or flanges | $\frac{l_s}{480}$ | $\frac{l_s}{500}$ or 8 mm whichever is the lesser | $\frac{a}{400}$ for 1st longitudinal stiffener | |
| | $\delta_s^{(+)}$ | $\frac{l_s}{900}$ or 2 mm whichever is the greater $G=l_s$ | | | | |
| | δ_s | for flats; $\frac{60}{b_c} \left(\frac{G}{1000}\right)^2$ for bulb flats; $\frac{50}{b_c} \left(\frac{G}{1000}\right)^2$ for angles; $\frac{50}{b_c} \left(\frac{G}{1000}\right)^2$ for tees; $\frac{60}{b_c} \left(\frac{G}{1000}\right)^2$ Except where $b > 3d_s$ for flats $b > 4d_s$ for bulb flats $b > 6d_s$ for angles and tees: for flats; $\frac{60}{b_c} \left(\frac{d_s}{250}\right)^2$ over gauge length $G=3d_s$ for bulb flats; $\frac{50}{b_c} \left(\frac{d_s}{200}\right)^2$ over gauge length $G=4d_s$ for angles; $\frac{50}{b_c} \left(\frac{d_s}{160}\right)^2$ over gauge length $G=6d_s$ for tees; $\frac{60}{b_c} \left(\frac{d_s}{160}\right)^2$ over gauge length $G=6d_s$ in no case less than 1.5 mm | 4.8 mm or $\frac{0.159D}{144\sqrt{T}}$ m whichever is the greater | | | |
| TRANSVERSE STIFFENER | δ_t | the same above | $\frac{l_s}{240}$ | the same above | $\frac{b_s}{400}$ | the same above |

* ÖNORM B4600/7, Stahlbau, Ausführung der Stahltragwerke, 1. Aug. 1975
 ÖNORM B4602, Stahlbau, Strassen brücken, 1. Aug. 1975

a: Panel length
 t: Thickness
 b: Panel width
 d_s : Height of rib



Before discussing the results of the measurements, it might be of value to see how the initial imperfections are limited by the design specifications in various countries. This is simply shown by Table 1. These limitations will be quoted afterwards when the results of the statistical analyses are discussed.¹⁾⁻⁵⁾

The main purposes of the proposed study include the following:

- (1) firstly, to investigate the statistical distributions of important design parameters characterizing the web plate systems,
- (2) secondly, to consider and determine the reasonable limiting values of the initial imperfections with a view to finding more reliable background to the design specifications,

Table 2. The geometric and mechanical parameters of the webplates.

| GEOMETRIC PARAMETERS | | MECHANICAL PARAMETERS | |
|-----------------------------|--------------------------------------|---|----------------------------------|
| <i>Aspect ratio of</i> | | <i>Young's modulus</i> | $E=21000 \text{ kg/mm}^2$ |
| web | $\alpha_w=a H_0$ | <i>Shear modulus</i> | $G= 8000 \text{ kg/mm}^2$ |
| h. stiffener | $\alpha_{hs1}=a b_{hs1}$ | <i>Poisson's ratio</i> | $\nu=0.3$ |
| | $\alpha_{hs2}=a b_{hs2}$ | <i>Flexural rigidity</i> | $D=\frac{Et_w^3}{12(1-\nu^2)}$ |
| v. stiffener | $\alpha_{vs}=H_0 b_{vs}$ | <i>Yielding strain of</i> | |
| u. flange | $\alpha_{uf}=a b_{uf}$ | web | $\epsilon_w=\sigma_{Yw} E$ |
| l. flange | $\alpha_{lf}=a b_{lf}$ | h. stiffener | $\epsilon_{hs1}=\sigma_{Yhs1} E$ |
| | | | $\epsilon_{hs2}=\sigma_{Yhs2} E$ |
| <i>Slenderness ratio of</i> | | v. stiffener | $\epsilon_{vs}=\sigma_{Yvs} E$ |
| web | $\beta_w=H_0 t_w$ | u. flange | $\epsilon_{uf}=\sigma_{Yuf} E$ |
| h. stiffener | $\beta_{hs1}=b_{hs1} t_{hs1}$ | l. flange | $\epsilon_{lf}=\sigma_{Ylf} E$ |
| | $\beta_{hs2}=b_{hs2} t_{hs2}$ | | |
| v. stiffener | $\beta_{vs}=b_{vs} t_{vs}$ | <i>Relative flexural stiffness of</i> | |
| u. flange | $\beta_{uf}=b_{uf} t_{uf}$ | h. stiffener | $\tau_{hs1}=EI_{hs1} H_0D$ |
| l. flange | $\beta_{lf}=b_{lf} t_{lf}$ | | $\tau_{hs2}=EI_{hs2} H_0D$ |
| <i>Relative position of</i> | | v. stiffener | $\tau_{vs}=EI_{vs} H_0D$ |
| h. stiffener | $\eta_1=(H_2+H_3) H_0$ | u. flange | $\tau_{uf}=EI_{uf} H_0D$ |
| | $\eta_2=H_3 H_0$ | l. flange | $\tau_{lf}=EI_{lf} H_0D$ |
| <i>Ratio of</i> | | <i>St. Venant's torsional rigidity of</i> | |
| h. stiffener area | $\delta_{hs1}=t_{hs1}b_{hs1} t_wH_0$ | h. stiffener | $\chi_{hs1}=GJ_{hs1} EI_{hs1}$ |
| | $\delta_{hs2}=t_{hs2}b_{hs2} t_wH_0$ | | $\chi_{hs2}=GJ_{hs2} EI_{hs2}$ |
| v. stiffener area | $\delta_{vs}=t_{vs}b_{vs} t_wH_0$ | v. stiffener | $\chi_{vs}=GJ_{vs} EI_{vs}$ |
| u. flange area | $\delta_{uf}=t_{uf}b_{uf} t_wH_0$ | u. flange | $\chi_{uf}=GJ_{uf} EI_{uf}$ |
| l. flange area | $\delta_{lf}=t_{lf}b_{lf} t_wH_0$ | l. flange | $\chi_{lf}=GJ_{lf} EI_{lf}$ |
| | | where σ_{Yw} : minimum yielding stress | |
| | | GJ_s : torsional rigidity | |
| | | $GJ_s=G\frac{1}{3}\sum b_it_i^3$ | |
| | | b_i : width t_i : thickness | |

(3) thirdly, to obtain the distribution of the ultimate strength of the web plates through the substitution of the actual initial imperfections into the appropriate equations representing the strength in terms of the imperfections and the design parameters.

The general outline of the proposed study is illustrated in Fig. 3. The statistical analyses were performed mainly by SPSS. SPSS refers to the Statistical Package for Social Sciences.⁶⁾ The subprograms of SPSS used herein are FREQUENCIES to find the probability distribution functions, SCATTERGRAM to find the correlations among the variables, and CLUSTER to classify the variables in certain groups.

2. Design Parameters

The design parameters of the webplates shown in Fig. 1 can be classified into geometric and mechanical parameters, as shown in Table 2.⁷⁾

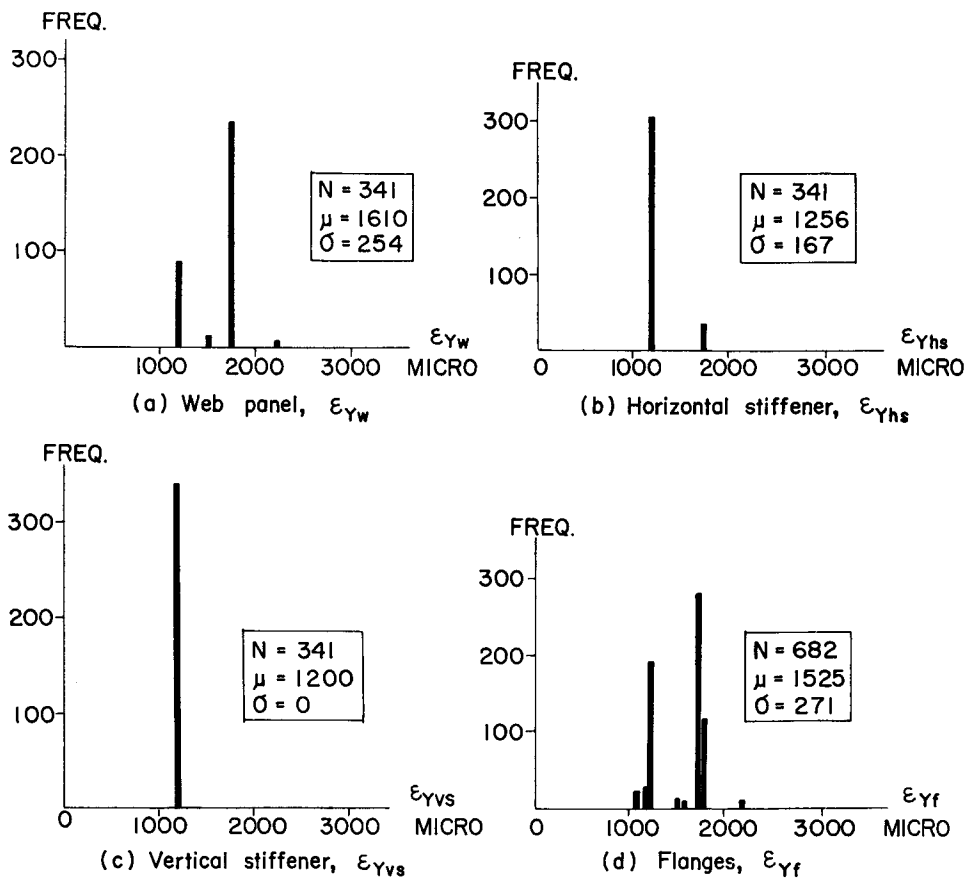


Fig. 4. The frequency distributions of the yielding strains.

Those parameters characterizing the webplates should be conveniently non-dimensionalized so that general and versatile conclusions can be drawn from the analyses.

Fig. 4 illustrates the frequency distributions of the yielding strains, ϵ_{yw} , ϵ_{yhs} ,

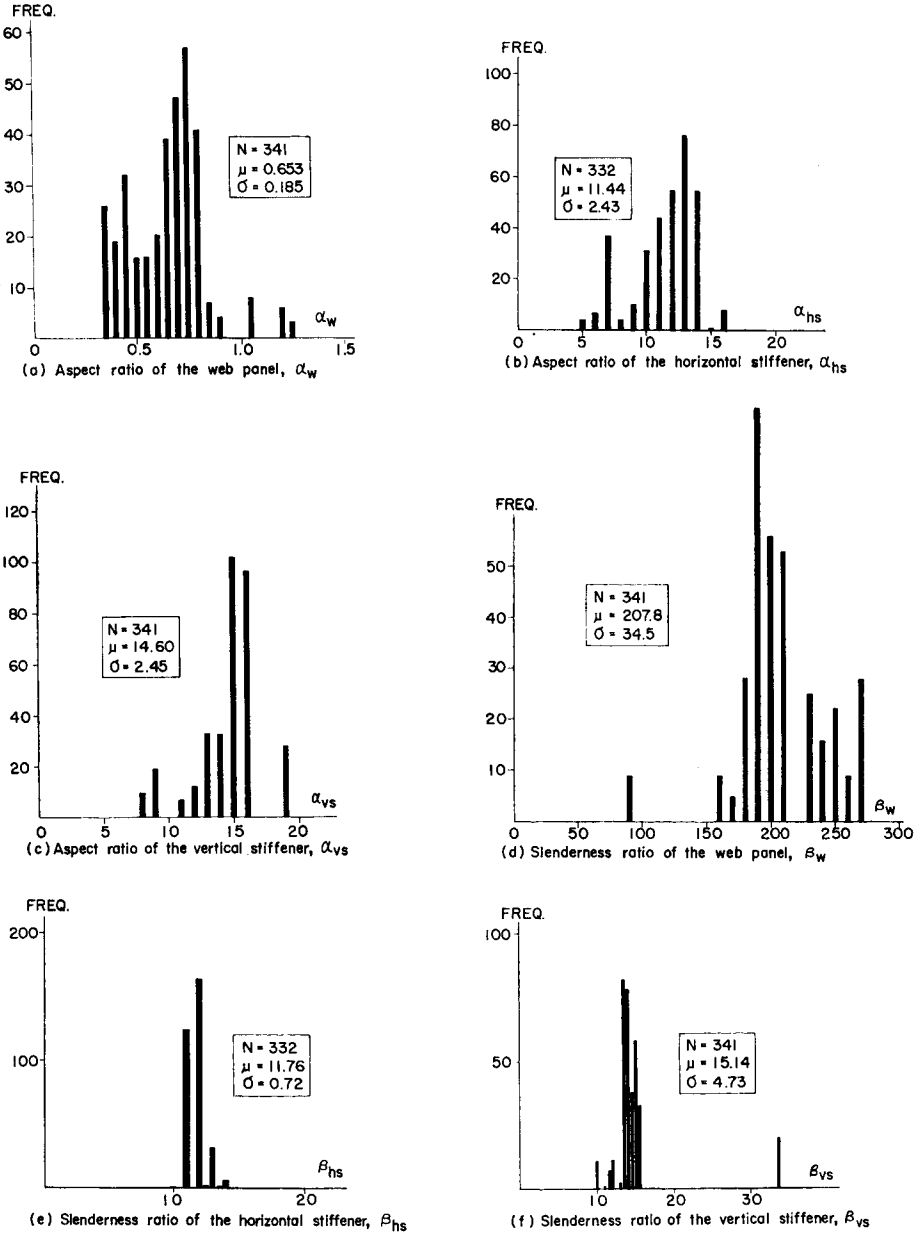


Fig. 5. The frequency distributions of the aspect ratios and the slenderness ratios.

$\epsilon_{\gamma_{vs}}$, and ϵ_{γ_f} , of the web panel, horizontal stiffener, vertical stiffener and the flanges, taking into account the variation of the yielding stresses of steel using different thicknesses, respectively. These simply represent what kinds of steel are being used. It is interesting to note that the vertical stiffeners are exclusively made of SS41.

Fig. 5 illustrates the frequency distributions of the aspect ratios, $\alpha_w, \alpha_{hs}, \alpha_{vs}$, and the slenderness ratios, $\beta_w, \beta_{hs}, \beta_{vs}$, of the web panel, horizontal stiffener and vertical stiffener, respectively.

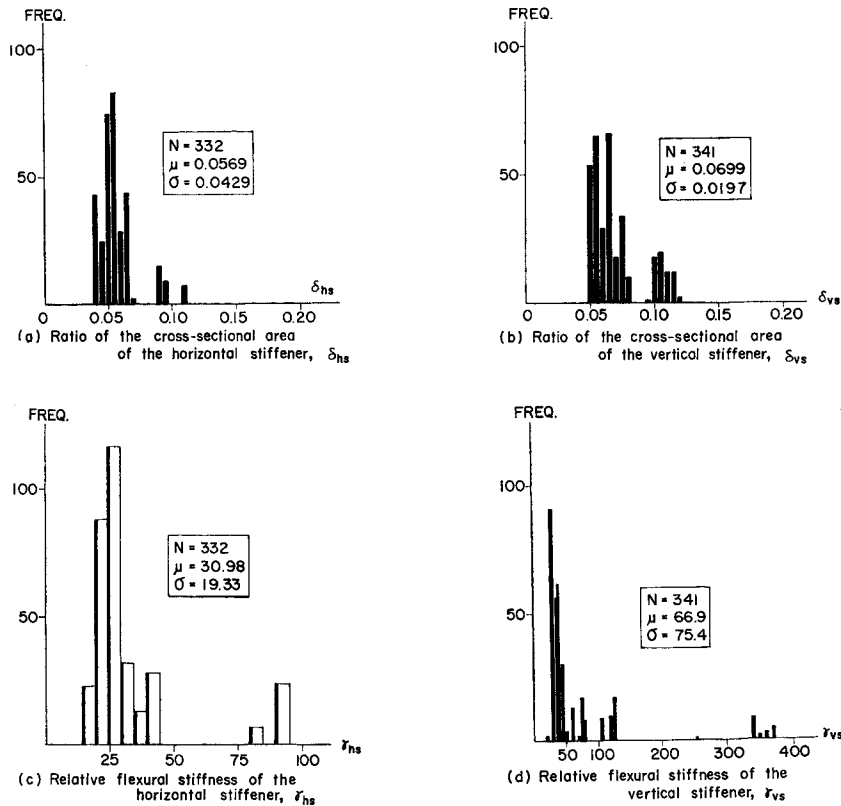


Fig. 6. The frequency distributions of the ratios of the cross-sectional area and the relative flexural stiffnesses.

Moreover, Fig. 6 illustrates those of the ratios of the cross-sectional area, δ_{hs}, δ_{vs} , and the relative flexural stiffnesses, γ_{hs}, γ_{vs} , of the horizontal and vertical stiffeners, respectively.

In addition to these, a correlation analysis was performed among various parameters to know how the parameters are related to each other. From this correlation analysis, the following observations can be made. Firstly, in each of the

horizontal and vertical stiffeners, the upper and lower flanges, the ratio of the cross-sectional area, δ , the moment of inertia, I , and the relative flexural stiffness, γ , are found closely correlated to each other as can be easily imagined. Secondly, in each of the horizontal and vertical stiffeners, not very strong correlations are found between α and β . Their correlation coefficients are found to be -0.251 and -0.541 , respectively. Thirdly, in the upper and lower flanges, α and β are found to be closely correlated: the correlation coefficients are found to be -0.878 and -0.800 , for the upper and lower flanges, respectively.

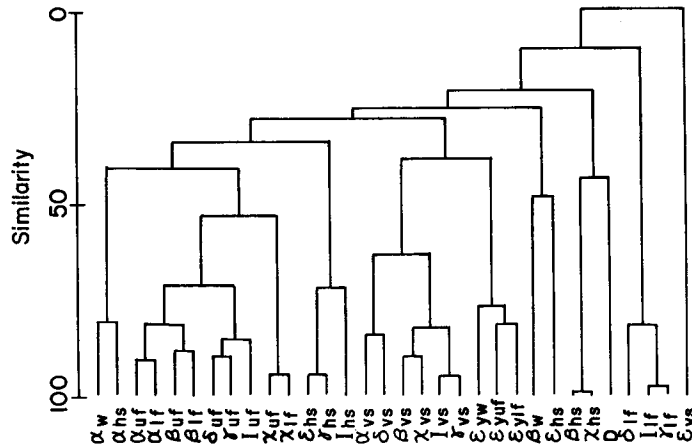


Fig. 7. The correlations among the design parameters. Dendrograms through cluster analysis.

The correlations among the design parameters can also be investigated by dendrograms through the CLUSTER analysis.^{8,9)} The results are summarized in Fig. 7. Firstly, it can be seen that the geometric and mechanical parameters form different clusters. Secondly, although the aspect ratio and the slenderness ratio of the flanges are similar, those of the vertical stiffeners form a different cluster.

3. Initial Imperfections

In these days, high-tension bolts and welding are widely used for the connections of steel members. However, during welding in particular, initial geometrical imperfections and the residual stresses are known to occur. Thus in general steel structures can be thought to be subjected to considerable initial deflections of certain shapes and residual stresses.

The initial imperfections may be sometimes better treated statistically, rather than being treated only deterministically, since they are influenced by so many

uncertain factors.

The geometrical imperfections and the residual stresses are generally referred to as the initial imperfections. In spite of the fact that the residual stresses are considered to be equally important, the considerations herein are limited to the initial displacements, since only a few data are available for the statistical analysis of the residual stresses.

The actual initial displacements have complex shapes in general. However, these shapes may be conveniently represented by the modal analysis utilizing six independent shapes defined as 'modes', as illustrated in Fig. 8, after the appropriate elimination of the rigid body motions. Modes from 1 to 6 are referred to as the 'Cylindrical bending mode (1)', 'Bending and twisting mode (1)', 'Cylindrical bending mode (2)', 'Bending and twisting mode (2)', 'Simple twisting mode', and 'Plate bending mode', respectively.¹⁾ These modes may be identified by the subscripts on the displace-

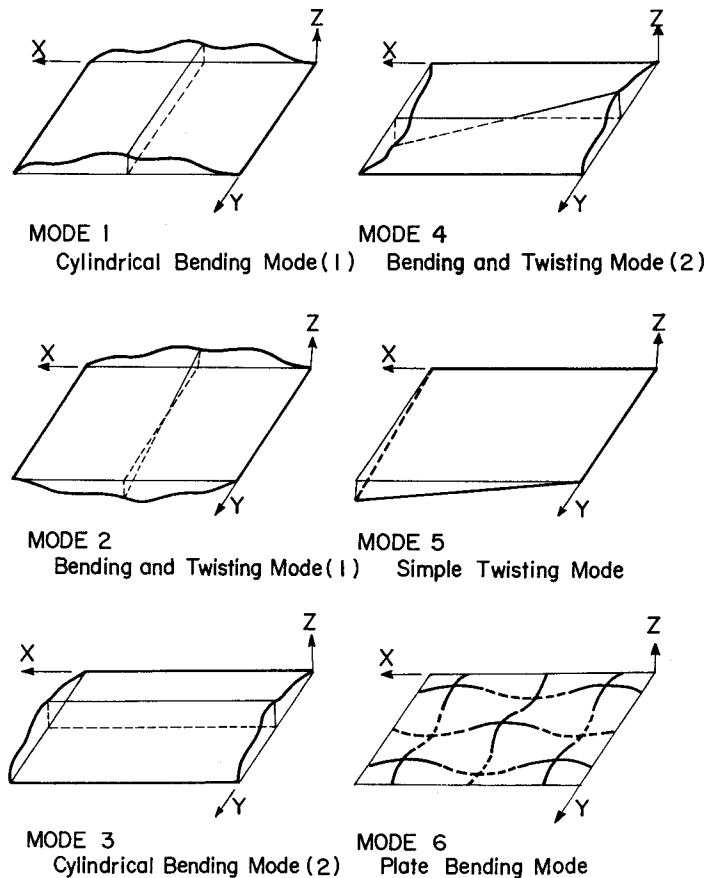


Fig. 8. Six independent modes considered.

ment components, u , v , and w , corresponding to the x -, y -, and z -directions, respectively, referring to the coordinate system defined in Fig. 1. Thus, for example, w_1 designates the vertical displacement of the 'cylindrical bending mode (1)'.

Furthermore, the term 'harmonics' will be used to distinguish the many wave shapes belonging to the same mode. The harmonics generally designate the number of half waves.

Fig. 9 shows the frequency distribution of the initial twist, $|v_5|/H_0$, of the 1st

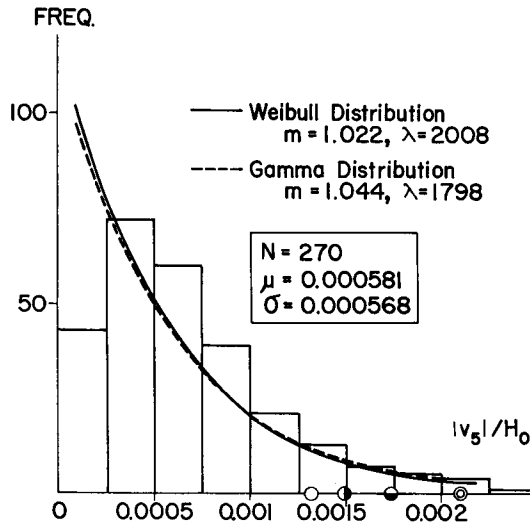


Fig. 9. The frequency distribution of the absolute initial twisting displacement of the web panel, $|v_5|/H_0$.

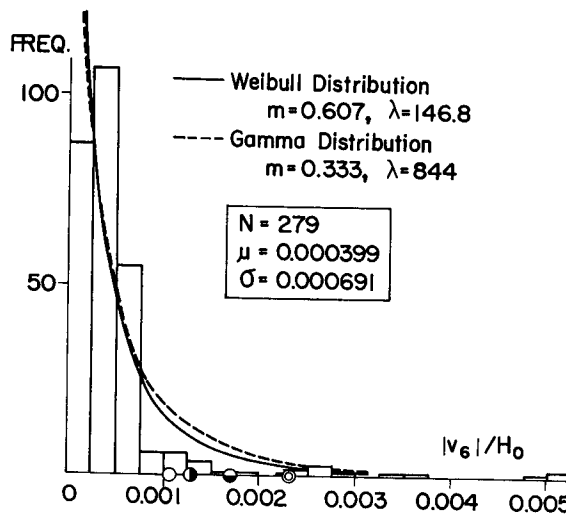


Fig. 10. The frequency distribution of the absolute initial horizontal displacement of the web panel, $|v_6|/H_0$. Harmonic 1×1 .

web panel.

Fig. 10 shows the frequency distribution of the initial horizontal displacement, $|v_6|/H_0$, of the 1st web panel of harmonic 1×1 .

Fig. 11 shows the frequency distribution of the initial horizontal displacement, $|v_1|/a$, of the horizontal stiffener of the 1st harmonic.

Fig. 12 shows the frequency distribution of the initial horizontal displacement, $|v_1|/H_0$, of the vertical stiffener of the 1st harmonic.

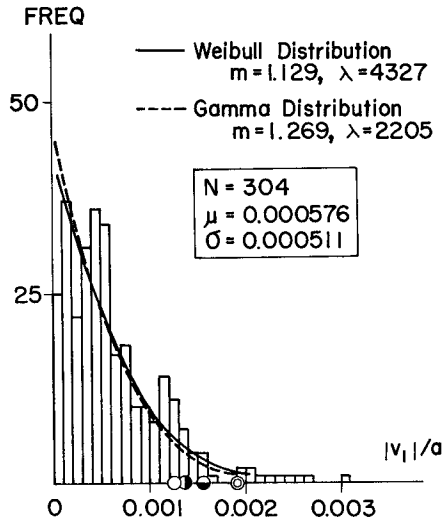


Fig. 11. The frequency distribution of the absolute initial horizontal displacement, $|v_1|/a$. 1st harmonic of horizontal stiffener.

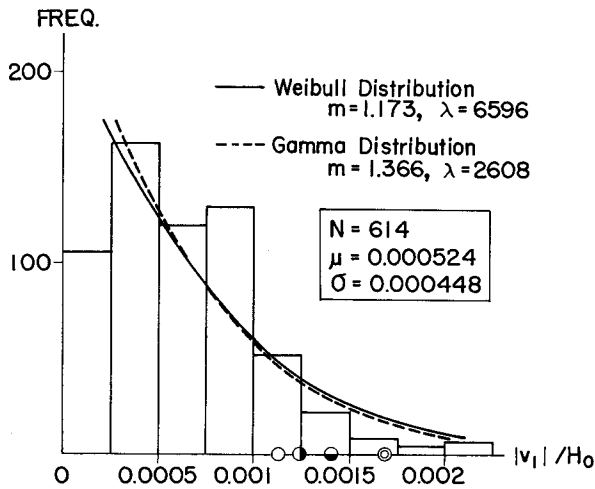


Fig. 12. The frequency distribution of the absolute initial horizontal displacement, $|v_1|/H_0$. 1st harmonic of vertical stiffener.

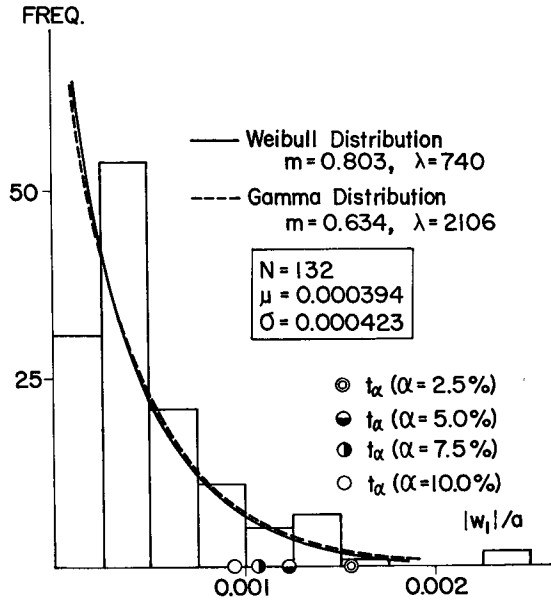


Fig. 13. The frequency distribution of the absolute initial vertical displacement, $|w_1|/a$. 1st harmonic of horizontal stiffener.

Furthermore, Fig. 13 shows the frequency distribution of the initial vertical displacement, $|w_1|/a$, of the horizontal stiffener of the 1st harmonic.

A good fitting of the probability function can be checked by the linearity of the plotted values in the probability papers, or by the χ^2 -test, or by the Kolmogorov-Smirnov test.¹⁰ In this study, this check was mostly performed by the χ^2 -tests.

Weibull¹¹) and Gamma distributions are generally known to be well fitted, and thus they were used in the proposed study to predict the probabilities of exceedance and non-exceedance of the initial displacements, and the imperfection sensitivity, respectively.

The probability density function of the Weibull distribution is given by

$$f(t) = \begin{cases} 0 & (t \leq 0) \\ \lambda m t^{m-1} \exp(-\lambda t^m) & (t > 0) \end{cases} \quad (1)$$

and the expected value, $E(t)$, and the variance, $V(t)$, can be obtained respectively by

$$E(t) = \lambda^{-1/m} \Gamma\left(\frac{m+1}{m}\right) \quad (2)$$

$$V(t) = \lambda^{-2/m} \left\{ \Gamma\left(\frac{m+2}{m}\right) - \Gamma\left(\frac{m+1}{m}\right)^2 \right\} \quad (3)$$

where $\Gamma(t)$ is a Gamma function

$$\Gamma(t) = \int_0^{\infty} u^{t-1} \exp(-u) du \quad (4)$$

The Weibull distribution may be characterized by its versatility being widely used on account of having two independent parameters m and λ , that is, two degrees of freedom.

Let us consider the relationship between the probability of exceedance of the Weibull distribution, α , and the value of the variables corresponding to α . The following results can be easily obtained.

$$\alpha = \int_{t_{\alpha}}^{\infty} f(t) dt = \exp(-\lambda t_{\alpha}^m) \quad (5)$$

$$t_{\alpha} = (\ln \alpha^{-1/\lambda})^{1/m} \quad (6)$$

Next, let us consider the Gamma distribution which is two-degree-of-freedom as in the case of the Weibull distribution. The probability density function of the Gamma distribution is defined as follows.

$$f(t) = \begin{cases} 0 & (t \leq 0) \\ \lambda^m t^{m-1} \exp(-\lambda t) / \Gamma(m) & (t > 0) \end{cases} \quad (7)$$

where $\Gamma(m)$ is a Gamma function. Its expected value, $E(t)$, and variance, $V(t)$, are given respectively by

$$E(t) = m/\lambda \quad (8)$$

$$V(t) = m/\lambda^2 \quad (9)$$

Let the probability of exceedance of this Gamma distribution be α , and the value of the variable corresponding to this α be t_{α} , then the relation between α and t_{α} is given by

$$\alpha = \frac{1}{\Gamma(m)} \int_{t_{\alpha}}^{\infty} \lambda^m t^{m-1} \exp(-\lambda t) dt \quad (10)$$

Substituting the prescribed mean value and variance into Eqs. (2) and (3) in the case of the Weibull distribution, or into Eqs. (8) and (9) in the case of the Gamma distribution, parameters m and λ can be obtained by the Regula-Falsi method in the case of the Weibull distribution, and can be directly obtainable in the case of the Gamma distribution.

In Figs. 9 to 13, the values of parameters m and λ of the Weibull and Gamma

Table 3. The results of the statistical analysis of the non-dimensionalized initial imperfections.

| KINDS OF INITIAL IMPERFECTIONS | MEAN VALUE μ | STANDARD DEVIATION σ | VARIABLE VALUE CORRESPONDING TO | | | | | | % PROBABILITY OF EXCEEDANCE CORRESPONDING TO VARIABLE VALUE (IN TERMS OF H_0 or a) | | | | |
|---|---------------------|--------------------------------|---------------------------------|------------------|------------------|-------------------------|------------------|------------------|---|------------------|------------------|-----------------|-----------------|
| | | | $\sigma + \mu$ | $\mu + 2\sigma$ | $\mu + 3\sigma$ | % PROBLTY OF EXCEEDANCE | | | $\frac{1}{250}$ | $\frac{1}{1200}$ | $\frac{1}{1000}$ | $\frac{1}{900}$ | $\frac{1}{480}$ |
| | | | | | | 2.5% | 5.0% | 10.0% | | | | | |
| Twist of Panel $ v_5 /H_0$ | $\frac{1}{1724}$ | $\frac{1}{1754}$ | $\frac{1}{870}$ | $\frac{1}{581}$ | $\frac{1}{435}$ | $\frac{1}{476}$ | $\frac{1}{588}$ | $\frac{1}{769}$ | 0.08 | ... | ... | ... | ... |
| Horz. Displ. Horz. Stffnr. 1st Mode: $ v_1 /a$ | $\frac{1}{1724}$ | $\frac{1}{1961}$ | $\frac{1}{917}$ | $\frac{1}{625}$ | $\frac{1}{476}$ | $\frac{1}{526}$ | $\frac{1}{625}$ | $\frac{1}{769}$ | ... | 23.58 | 16.95 | 13.55 | 1.72 |
| Horz. Displ. Vertical Stffnr. 1st Mode: $ v_1 /H_0$ | $\frac{1}{1923}$ | $\frac{1}{2222}$ | $\frac{1}{1031}$ | $\frac{1}{704}$ | $\frac{1}{535}$ | $\frac{1}{588}$ | $\frac{1}{714}$ | $\frac{1}{909}$ | ... | 19.87 | 13.51 | 10.38 | 0.88 |
| Horz. Displ. Web Panel Mode $1 \times 1: v_6 /H_0$ | $\frac{1}{2500}$ | $\frac{1}{1449}$ | $\frac{1}{917}$ | $\frac{1}{562}$ | $\frac{1}{405}$ | $\frac{1}{435}$ | $\frac{1}{625}$ | $\frac{1}{909}$ | 0.58 | ... | ... | ... | ... |
| Horz. Displ. Web Panel Mode $1 \times 2: v_6 /H_0$ | $\frac{1}{7692}$ | $\frac{1}{3571}$ | $\frac{1}{2439}$ | $\frac{1}{1449}$ | $\frac{1}{1031}$ | $\frac{1}{1111}$ | $\frac{1}{1667}$ | $\frac{1}{2500}$ | 0.02 | ... | ... | ... | ... |
| Horz. Displ. Tensn. Flange $ v_1 /a$ | $\frac{1}{1754}$ | $\frac{1}{1563}$ | $\frac{1}{826}$ | $\frac{1}{541}$ | $\frac{1}{400}$ | $\frac{1}{435}$ | $\frac{1}{556}$ | $\frac{1}{714}$ | ... | 22.99 | 17.68 | 14.88 | 3.49 |
| Horz. Displ. Compr. Flange $ v_1 /a$ | $\frac{1}{1053}$ | $\frac{1}{361}$ | $\frac{1}{269}$ | $\frac{1}{154}$ | $\frac{1}{108}$ | $\frac{1}{137}$ | $\frac{1}{227}$ | $\frac{1}{417}$ | ... | 22.51 | 20.00 | 18.61 | 11.23 |
| Vertical Displ. Horz. Stffnr. 1st Mode: $ w_7 /a$ | $\frac{1}{2564}$ | $\frac{1}{2381}$ | $\frac{1}{1235}$ | $\frac{1}{813}$ | $\frac{1}{606}$ | $\frac{1}{667}$ | $\frac{1}{833}$ | $\frac{1}{1111}$ | ... | 8.22 | 5.54 | 4.29 | 0.54 |

distributions are shown. Fitted Weibull distributions are designated by the solid lines; while, the Gamma distributions are designated by the broken lines. In these figures, the values of variables corresponding to the following value of the probability of exceedance, α , are marked with different circles: 2.5%, 5%, 7.5%, and 10%.

Table 3 shows the results of the statistical analysis of the non-dimensionalized initial imperfections. In this table, μ and σ refer to the mean value and the stan-

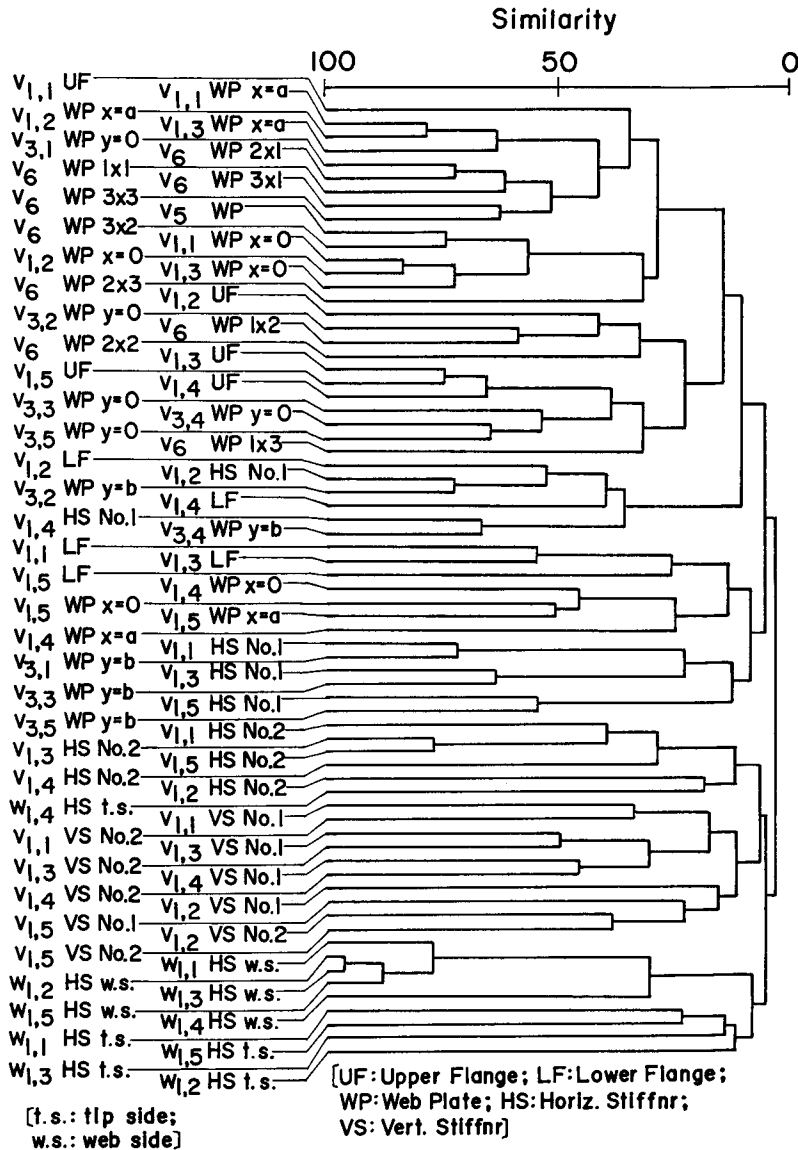


Fig. 14. The dendrogram among the 'modes' and the 'harmonics' of the initial imperfections.

dard deviation for each of the initial imperfections, respectively. Also shown are $\mu + \sigma$, $\mu + 2\sigma$, $\mu + 3\sigma$, and the values of the initial imperfections corresponding to the probability of exceedance, 2.5%, 5%, 7.5%, and 10%, respectively. In addition, the percentage probabilities of exceedance are shown for certain prescribed values of imperfections such as those limited by Japanese Specifications on Highway Bridges, AASHTO, IDWR, ÖNORM, and DAST: 1/250, 1/1200, 1/1000, 1/900, and 1/480.¹⁾⁻⁵⁾

Take $H_0/250$ as the limiting value of the initial imperfection for the web panel, then, the corresponding probability of exceedance will be found to be no greater than 1%. On the other hand, let the limiting value of the initial imperfection of the horizontal stiffener, vertical stiffener, and flange be $a/1000$, or $H_0/1000$, then the corresponding probability of exceedance will be found as high as 14% to 20%.

Fig. 14 presents the dendrogram among the 'modes' and 'harmonics' of various initial imperfections to show their correlations. The first subscript refers to the mode, and the second one after a comma refers to the harmonic, respectively. It will be seen from this figure that the correlations among the harmonics in each of the modes are more significant than those among the different modes.

Furthermore, a correlation analysis among the initial imperfections and the design parameters was conducted. The results, however, show that the correlation is not very strong.

4. Relation Between Initial Imperfections and Ultimate Strength

The ultimate strength can be estimated by the theoretical equations relating initial imperfections to the ultimate strength. Then, the probability models can be obtained by fitting the Weibull and Gamma distributions to the frequency distributions of the ultimate strength. The results can be used for determining the limiting values of the imperfections for the design purposes.

Today, although there seem to be many equations to compute the ultimate strength of webs, it was found from a literature survey that only the following equations are available to take into account the effect of the imperfections upon the load carrying capacity of web plate system. The first is the equation to compute the strength against the local torsional buckling of the horizontal stiffener derived by Chatterjee and Dowling. The second is the equation to compute the local compressive ultimate strength of the horizontal stiffener considering the appropriate effective area of webs.

Chatterjee and Dowling considered such a mechanical model for torsional

buckling, as shown in Fig. 15.¹²⁾ This model is simply supported along three edges and free at the other edge. Let the load carrying capacity be defined as the load at which plastic deformation is initiated along the supported edges, then, it is given by

$$K_{su} = \frac{\sigma_{au}}{\sigma_{Ys}} = \frac{m_f - 1}{2.6r^2 m_f} + 0.658 s^2 (m_f^2 - 1) \quad (11)$$

and

$$3.849 r^2 s^2 m_f^2 - \frac{1}{m_f} = 2.6 r^2 + 3.849 r^2 s^2 - 1 \quad (12)$$

where r and s are given respectively by

$$r = \frac{b_s}{t_s} \sqrt{\frac{\sigma_{Ys}}{E}}; \quad s = \frac{\delta}{a} \sqrt{\frac{E}{\sigma_{Ys}}} \quad (13)$$

In these equations, σ_{au} refers to the average stress of the panel at the ultimate load, and σ_{Ys} refers to the yielding stress of the stiffener. Furthermore, b_s , t_s , a

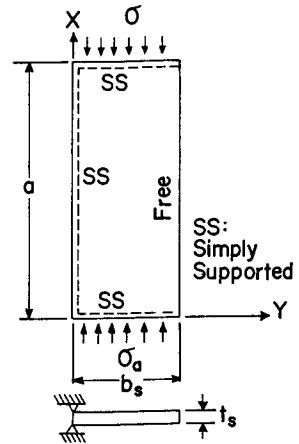


Fig. 15. The mechanical model for local torsional buckling of the horizontal stiffener.

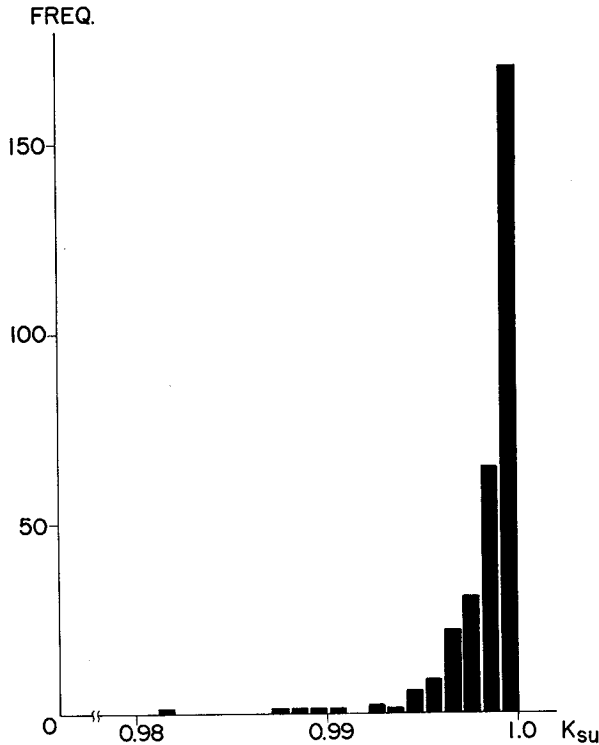


Fig. 16. The frequency distribution of the imperfection sensitivity, K_{su} .

and δ refer to the width of the stiffener, its thickness, its length and the maximum magnitude of the stiffener distortion, respectively.

Solving Eq. (12) for m_f by the Newton-Raphson method, and substituting m_f into Eq. (11) yield the value of K_{su} , that is, the imperfection sensitivity.

Fig. 16 indicates the frequency distribution of K_{su} . The result shows that the mean value of the imperfection sensitivity is 99.9%, and the maximum value is as high as 98%. This clearly indicates the fact that the initial vertical lateral displacements of horizontal stiffeners existing in the web plate systems have little influence upon the lateral buckling load.

What will most significantly affect the strength against the torsional buckling of the stiffener? To answer this question, correlation analyses are conducted. Fig. 17 shows the scattergram between K_{su} and s . This correlation coefficient is found to be -0.8735 . Thus, it can be seen that s , representing imperfection, has a much greater influence upon the imperfection sensitivity than any other factors, as can be easily expected.

Fig. 18 shows a mechanical model for compressive ultimate strength analysis. A portion of the webplate is assumed to collaborate with the horizontal stiffener in resisting the axial compression. The hatched area, that is, the stiffener and the

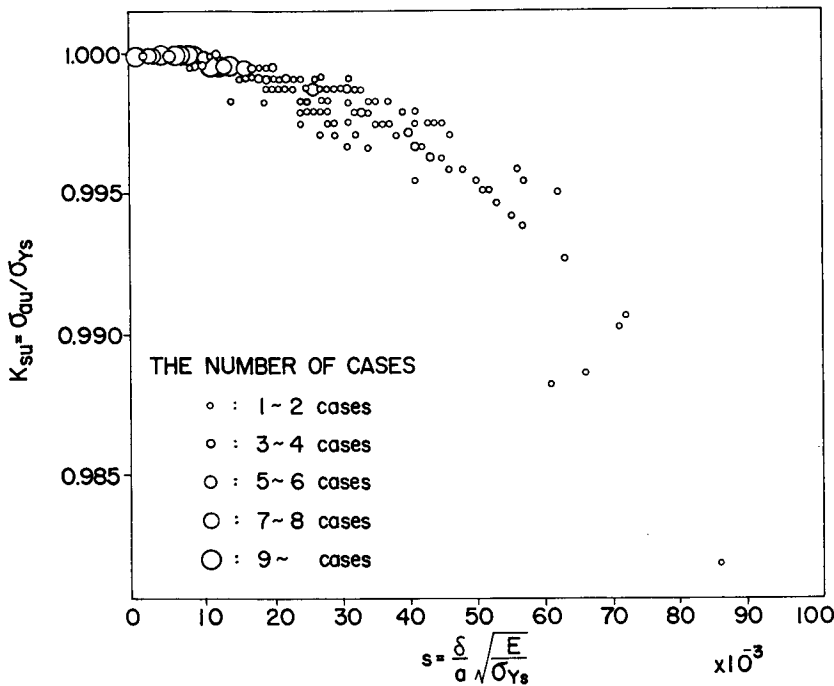


Fig. 17. The scattergram between K_{su} and s .

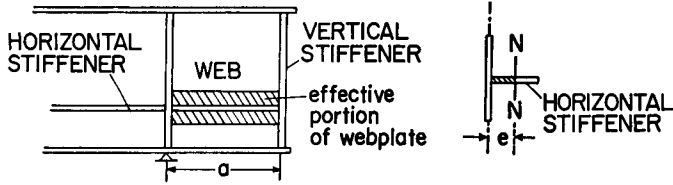


Fig. 18. The mechanical model of the equivalent column.

effective width of web being put together, is regarded as a compressed column with a T-cross section. The effective width of the web is assumed conveniently to be $24t_w$. Assume that this column is simply supported at both ends. Also, let v , σ_u , a , c and r designate the magnitude of initial deflection in the sine wave of the 1st harmonic, the ultimate axial compressive stress, the length of the stiffener, the edge distance and the radius of gyration of area, respectively. The ultimate strength is defined as the load at which the stiffener initiates plastic deformation at its tip side. The ultimate strength is obtained by the following nonlinear equation of the type of the Perry-Robertson formula:

$$\frac{\sigma_u}{\sigma_Y} = \left(1 + \frac{cv}{r^2} \frac{1}{1 - \lambda^2 \frac{\sigma_u}{\sigma_Y}} + \frac{ce}{r^2} \sec \frac{\pi}{2} \lambda \sqrt{\frac{\sigma_u}{\sigma_Y}} \right)^{-1} \quad (14)$$

where σ_Y , cv/r^2 , and ce/r^2 refer to the yielding stress, the non-dimensionalized initial imperfections and the non-dimensionalized eccentricity, respectively; while λ is referred to as the generalized slenderness ratio of the horizontal stiffener defined by

$$\lambda = \frac{a}{r} \sqrt{\frac{\sigma_Y}{\pi^2 E}} \quad (15)$$

This nonlinear transcendental equation can be solved by the Newton-Raphson method.

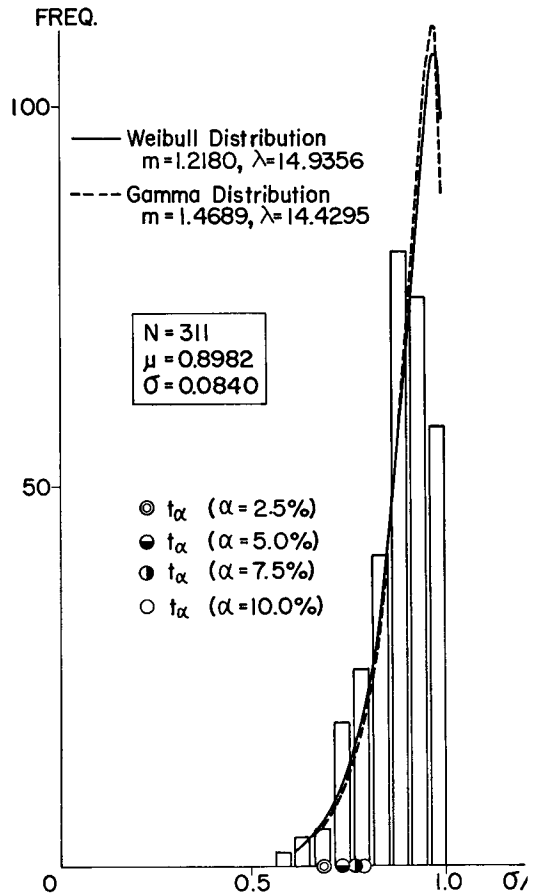


Fig. 19. The frequency distribution of the imperfection sensitivity, σ_u/σ_Y for $e=0$.

As yet, it would be quite difficult theoretically to determine how much of the eccentricity, e , should be considered. To simplify the problem, two cases are taken into consideration: In the first case, the eccentricity is assumed to be negligible, that is, $e=0$; and secondly, the eccentricity is assumed to be equal to the imperfection, that is, $e=v$.

Fig. 19 shows the frequency distribution of the imperfection sensitivity, σ_u/σ_Y , when $e=0$; while Fig. 20 shows that result when $e=v$. To be quite different from the case of torsional buckling of horizontal stiffener, the mean value of the imperfection sensitivity turns out to be 89.9%, and the minimum value is as low as 60% when $e=0$. These values are seen to decrease to 82.6%, and 45%, respectively, when $e=v$.

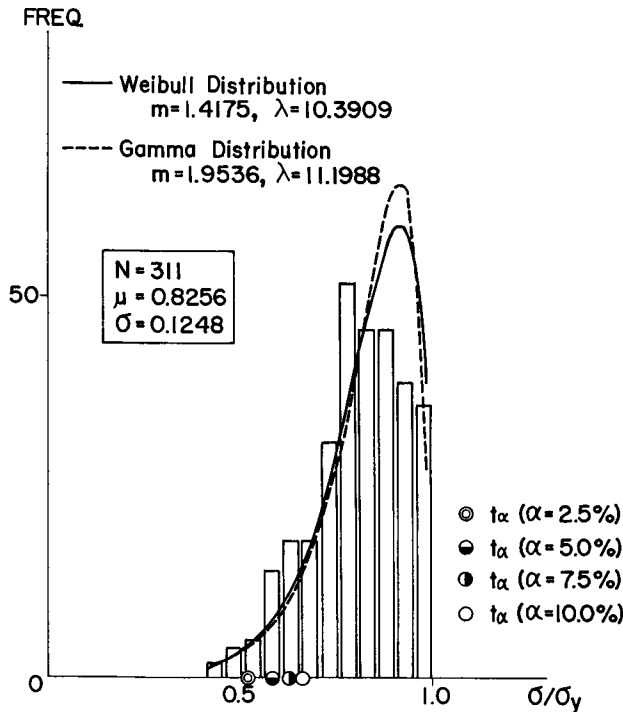


Fig. 20. The frequency distribution of the imperfection sensitivity, σ_u/σ_Y for $e=v$.

What will most significantly affect the imperfection sensitivity? To answer this question, a correlation analysis is conducted. Fig. 21 shows the scattergram between the imperfection sensitivity and the non-dimensionalized initial imperfection when $e=0$. Fig. 22 shows that result when $e=v$. From the comparison of the imperfection sensitivities shown in Figs. 21 and 22 with that shown in Fig. 17, it will be seen that this time, the ultimate load carrying capacity is far more sensi-

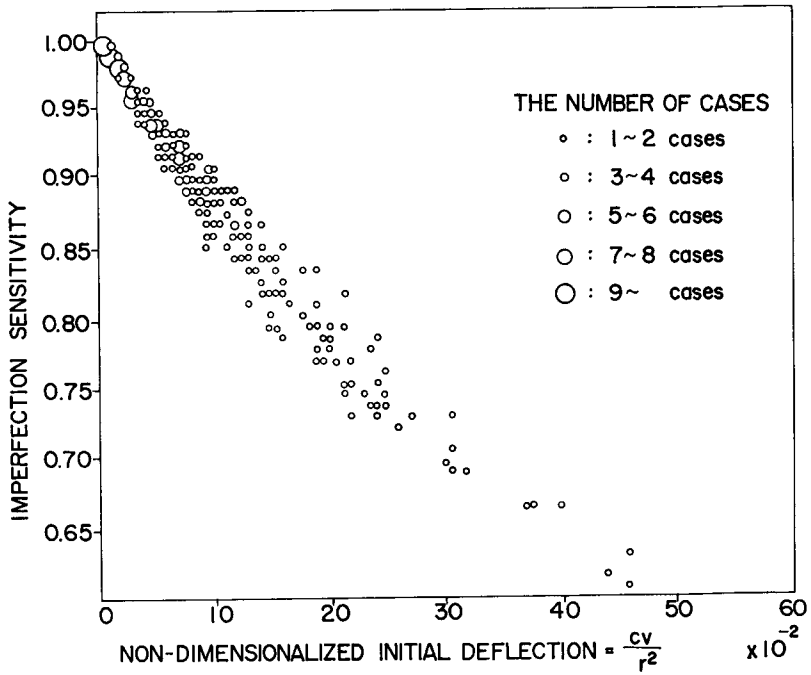


Fig. 21. The scattergram between the imperfection sensitivity and the non-dimensionalized initial imperfection for $\epsilon=0$.

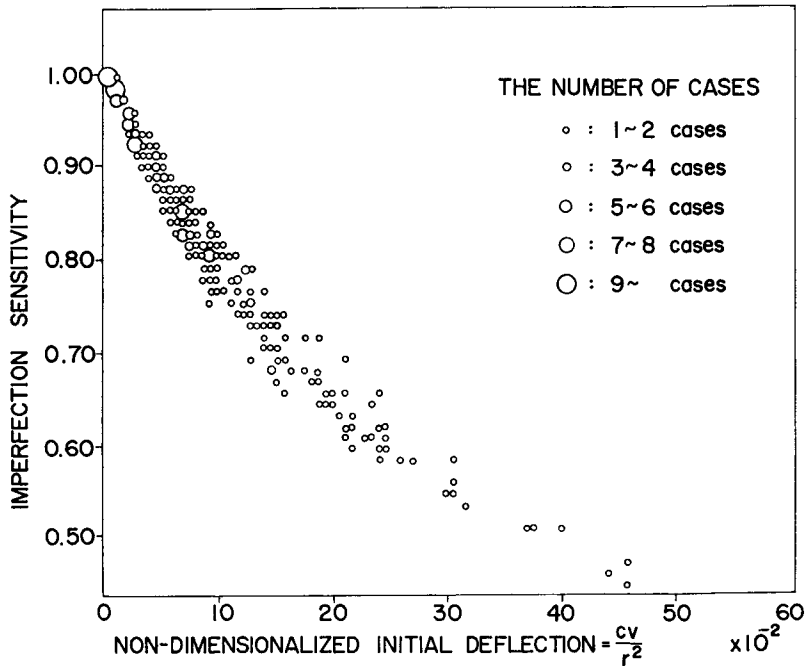


Fig. 22. The scattergram between the imperfection sensitivity and the non-dimensionalized initial imperfection for $\epsilon=v$.

tive to the imperfection. Furthermore, it will also be seen that the scatter of the sensitivity increases as the imperfection increases.

Following the same procedure as for the determination of the probability density function of the initial imperfections, the frequency distributions may be fitted by the Weibull and Gamma distributions for the load carrying capacity. It is to be noted this time, however, to consider the probability of non-exceedance for the ultimate strength, as compared with the probability of exceedance for the initial imperfections.

The value of the ultimate strength corresponding to a certain particular value of the probability of non-exceedance, α , will not necessarily correspond to the value of the imperfection corresponding to the probability of exceedance of the same value, α . This discrepancy may be attributed to the fact that the design parameters such as the slenderness ratio are also statistical variables, too.

In order to obtain a simple one-to-one correspondence between the ultimate strength and the initial imperfection, let us consider an ideal structure having the expected value of the generalized slenderness ratio of the horizontal stiffener, $\bar{\lambda}$. This value has been found to be:

$$\bar{\lambda} = \frac{a}{r} \sqrt{\frac{\sigma_Y}{\pi^2 E}} = 0.543$$

Let the expected value and the standard deviation of the non-dimensionalized initial imperfection, cv/r^2 , be designated by μ_i and σ_i ; while those of the imperfection sensitivity, σ_u/σ_Y , by μ_s and σ_s , respectively. Table 4 shows the values of the imperfection sensitivity, σ_u/σ_Y , corresponding to $\mu_i, \mu_i + \sigma_i, \mu_i + 2\sigma_i, \mu_i + 3\sigma_i$, and the probabilities of exceedance, 2.5%, 5%, and 10% of the imperfection, respectively, for the columns having an ideal slenderness ratio, $\bar{\lambda}$.

Now, let us assume that the slenderness ratio, λ , be a statistical variable, as it is. Upon substitution of this slenderness ratio, and the imperfection, the imper-

Table 4. The values of the imperfection sensitivity of the 'ideal' equivalent columns of the constant slenderness ratio.

$$\bar{\lambda} = 0.543$$

| THE VALUES OF σ_u/σ_Y CORRESPONDING TO CHARACTERISTIC VALUES OF cv/r^2 | | | | | | | | |
|--|-----------------------------|---------|--------------------|---------------------|---------------------|---------------------------|--------|--------|
| INITIAL IMPERFECTIONS: cv/r^2 | | | | | | PROBABILITY OF EXCEEDANCE | | |
| | | | | | | 2.5% | 5.0% | 10.0% |
| | | μ_i | $\mu_i + \sigma_i$ | $\mu_i + 2\sigma_i$ | $\mu_i + 3\sigma_i$ | | | |
| IMPERFECTION SENSITIVITY | $e=0$ | 0.8963 | 0.8170 | 0.7532 | 0.7002 | 0.7158 | 0.7535 | 0.7963 |
| | $e=v$ | 0.8127 | 0.6953 | 0.6115 | 0.5477 | 0.5660 | 0.6118 | 0.6671 |
| | $\frac{\sigma_u}{\sigma_Y}$ | | | | | | | |

Table 5. The values of the imperfection sensitivity of the equivalent columns.

| | Imperfection Sensitivity σ_u/σ_Y | | | | | | |
|-------|--|--------------------|---------------------|---------------------|-------------------------------|--------|--------|
| | | | | | PROBABILITY OF NON-EXCEEDANCE | | |
| | μ_s | $\mu_s - \sigma_s$ | $\mu_s - 2\sigma_s$ | $\mu_s - 3\sigma_s$ | 2.5% | 5.0% | 10.0% |
| $e=0$ | 0.8982 | 0.8142 | 0.7302 | 0.6462 | 0.6828 | 0.7326 | 0.7846 |
| $e=v$ | 0.8256 | 0.7008 | 0.5760 | 0.4511 | 0.5184 | 0.5842 | 0.6546 |

fection sensitivity can be evaluated in a statistical fashion. Table 5 shows the values of μ_s , $\mu_s - \sigma_s$, $\mu_s - 2\sigma_s$, $\mu_s - 3\sigma_s$, and the values of imperfection sensitivity corresponding to the probability of non-exceedance, 2.5%, 5%, and 10%.

From these tables, it will be seen firstly, that the ultimate strength corresponding to the eccentricity, $e=v$, is obviously smaller than $e=0$ by about 10%. Secondly, the values of the imperfection sensitivity corresponding to μ_i , $\mu_i + \sigma_i$ of the imperfection agree with the values of μ_s and $\mu_s - \sigma_s$ of the imperfection sensitivity fairly well. However, the values of the imperfection sensitivity corresponding to $\mu_i + 2\sigma_i$, $\mu_i + 3\sigma_i$ and the probabilities of exceedance of the imperfection, 2.5% and 5% are found to be greater than the values of $\mu_s - 2\sigma_s$, $\mu_s - 3\sigma_s$, and also the values of the imperfection sensitivities corresponding to the probabilities of non-exceedance, 2.5% and 5%, respectively. This observation may be thought quite reasonable if the variations of the slenderness ratio, λ , and the imperfections are taken into account. The variation of the imperfections has been shown by the frequency distribution in Fig. 11.

5. Conclusions and Acknowledgment

The main objective of this proposed study is to obtain the statistical characteristics of the actual imperfections of web plates of steel bridges, based on a broad survey by the Committee of Initial Deflection Measurement, IDMC, of the Society of Steel Construction of Japan, JSSC.

The following conclusions may be drawn:

1. The basic statistical frequency distributions of the design parameters and the imperfections are obtained.
2. The correlations among the design parameters and various imperfections are examined.
3. The probability functions of the initial imperfections are determined by the Weibull and Gamma distributions. The results are used to consider possible limiting values of the imperfections for practical use in design specifications.
4. The imperfection sensitivities are obtained by making use of the available

equations on the ultimate strength against the torsional buckling of the horizontal stiffeners and against the flexural buckling of the effective portion of the web plate and the horizontal stiffener.

5. The ultimate strength against the torsional buckling is found to be not strongly affected with such small imperfections as those actually measured. However, the imperfection sensitivity against the local flexural buckling of the effective column is found to be greatly affected by the imperfections.

6. The ultimate strength of the equivalent columns just mentioned above was subjected to further detailed statistical consideration. By use of the column strength equation of the Perry-Robertson type, the frequency distribution of the imperfection sensitivity is obtained. The probability density functions of the imperfection sensitivity were also determined by fitting the Weibull and Gamma distributions.

7. The values of the higher imperfection sensitivity of the equivalent column are found approximately coincident with those predicted through the frequency distribution of the imperfections, assuming the average deterministic value of the slenderness ratio.

8. The values of the smaller imperfection sensitivity, however, of the equivalent column are found to be less than those predicted through the frequency distribution of the imperfections, assuming the average slenderness ratio.

9. The current practice of adopting $H_0/250$ as the limiting value of the initial imperfection for the web panels of steel bridges may be considered as not being too strict.

10. The current practice adopting $a/1000$, or $H_0/1000$ as the limiting value of the stiffeners and the flanges, however, may be considered as being quite strict.

This study was financially assisted by a Grant-in-aid from the Ministry of Education. The authors are indebted to the Society of Steel Construction of Japan for the promotion of the study, and for all the assistance the society offered to them.

Last of all, appreciation is extended to Professor Sadao Komatsu of Osaka University for his general guidance and valuable suggestions.

Bibliography

- 1) JSSC and IDMC: Statistical Study on the Initial Deformations and the Ultimate Strengths of Steel Bridge Members, JSSC Journal, Vol. 16, No. 179, 1980. (in Japanese)
- 2) Japanese Association of Highways: Specifications for Highway Bridges, 1980. (in Japanese)
- 3) Interim Design and Workmanship Rules, Part I-IV, Report of the Committee-Appendix, Inquiry into the Basis of Design and Method of Erection of Steel Box Girder Bridges, Department of Environment, London, 1973.

- 4) AASHTO: Standard Specifications for Highway Bridges, American Association of State Highway and Transportation Officials, 1977.
- 5) Deutscher Ausschuss für Stahlbau-Richtlinien: DAST-Rit. 012, 1978.
- 6) Miyake, Ichiro and K. Yamamoto: SPSS Statistical Package I and II, Tohyo-Keizai-Shimpohsha, 1976. (in Japanese)
- 7) Inoue, Masahito: Studies on the Geometric Imperfections of Steel Structure -Web Plates-, Graduation Thesis, Kyoto University, 1979. (in Japanese)
- 8) Nakatani, Kazuo: Multivariate Analysis, Shinyosha, 1978. (in Japanese)
- 9) Mathematical Sciences: Cluster Analysis, Science Co., Ltd, No. 190, 1979. (in Japanese)
- 10) Ang, A. H-S and W.H. Tang: Probability Concepts in Engineering Planning and Design, Maruzen, 1977.
- 11) Kondo, J.: Applied Probability, Nikka-Giren, 1970. (in Japanese)
- 12) Chatterjee, S. and P.J. Dowling: The Design of Box Girder Compression Flanges, Steel Plated Structures, Crosby Lockwood Staples, London, 1977.